

# Different Biocompatibility and Radioprotective Activity of Squid Melanin Nanoparticles on Human Stromal Cells

Le-Na Thi Nguyen, Xuan-Hai Do, Hanh B. Pham, Dinh Duy-Thanh, Uyen Thi Trang Than, Thu-Huyen Nguyen, Van-Ba Nguyen, Duc-Son Le, Dinh-Thang Nguyen, Kien Trung Kieu, Phuc Trong Nguyen, Manh Duc Vu, Nghia Trung Tran, Thanh Lai Nguyen, Lien T H Nghiem, Toan D. Nguyen, Nga Thi Hang Nguyen, and Nhung-Thi My Hoang\*



Cite This: *ACS Omega* 2024, 9, 36926–36938



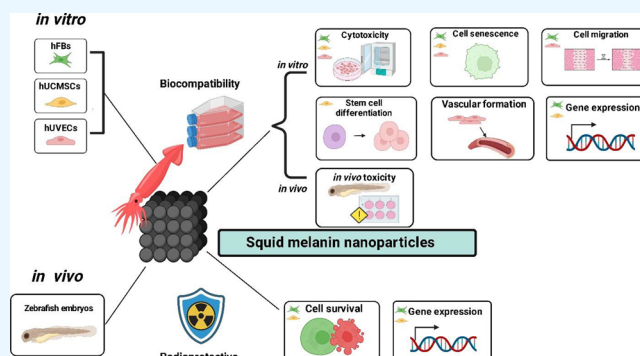
Read Online

ACCESS |

Metrics & More

Article Recommendations

**ABSTRACT:** Squid ink melanin nanoparticles (NPs) have recently been demonstrated to have a number of bioactivities; however, their biocompatibility has been poorly investigated. In this study, we aimed to evaluate the effects of this NP on stromal cells, including human fibroblasts (hFBs), human umbilical vein endothelial cells (hUVECs), and human umbilical cord-derived mesenchymal stem cells (UCMSCs), and on the development of zebrafish embryos under normal X-ray irradiation conditions. The NPs showed high biocompatibility with low cytotoxicity, no cell senescence induction, and no effect on cell migration in hFBs or cell differentiation in UCMSCs. Nonetheless, this compound prevented cell movement in UCMSCs and significantly suppressed tube formation in hUVECs at a dose of 25  $\mu\text{g}/\text{mL}$ . The NPs successfully penetrated the hUVECs but not the other two stromal cell types. The expression levels of functional genes involved in angiogenesis, apoptosis, antioxidant activity, and radiation sensitivity were altered in NPs subjected to hUVECs but were not affected in hFBs and UCMSCs. Melanin NPs significantly rescued cell viability and gene expression in irradiated hFBs and UCMSCs but not in hUVECs. In vivo treatments of zebrafish embryos showed that melanin NPs were nontoxic whether alone or under X-ray irradiation. These findings suggested that nanosized squid ink melanin had biocompatibility with selective stromal cells and was safe for early development.



## 1. INTRODUCTION

Melanin, including pheomelanin and eumelanin, is a group of color-producing substances that operate as a protective shield by absorbing harmful ultraviolet (UV) rays from solar radiation and collecting reactive oxygen species (ROS) to prevent DNA damage from reaching neighboring cells.<sup>1,2</sup> Melanin also plays a vital role in the innate immune system against bacterial and fungal pathogens.<sup>3</sup> Although melanin exhibits multifunctionality and intrinsic biocompatibility, it has poor water solubility, which can limit the potential application of this compound.<sup>2</sup> This has motivated scientists to develop a nanosized version of this compound called melanin nanoparticles (NPs).<sup>4–6</sup> Remarkably, a study in 2020 showed another capacity of using cuttlefish melanin nanoprobes for preoperative and intraoperative mapping of lymph nodes for cancer metastasis assessment.<sup>7</sup> Recently, melanin and melanin in the form of NPs have been reported to have the ability to protect against radiation.<sup>5,6,8–11</sup> In addition, Nguyen et al. demonstrated that squid melanin NPs induce the SKOV3 tumor-killing ability of X-rays.<sup>9</sup> Moreover, these NPs could protect the spleen from

radiation therapy in Swiss mice bearing 3LL tumors, consequently promoting antitumor immunity.<sup>8</sup>

While being an effective cancer treatment, radiotherapy may also damage healthy tissues and exert long-term effects on tissue regeneration, which in turn mainly involves several leading cell types, including mesenchymal stem cells (MSCs)<sup>12,13</sup> fibroblasts, and endothelial cells. MSCs maintain cellular homeostasis in the organism.<sup>14,15</sup> They are activated, divided, and differentiated following tissue damage into tissue-corresponding cells to alleviate injury.<sup>14,15</sup> Fibroblasts make up most of the stromal cells in all tissues. They play an essential role in tissue regeneration in response to tissue injury.<sup>16</sup>

**Received:** November 23, 2023

**Revised:** August 10, 2024

**Accepted:** August 13, 2024

**Published:** August 22, 2024



Another crucial step in the regeneration process is angiogenesis, which is primarily driven by endothelial cells. These cells were reported to be able to secrete angiocrine molecules and generate tissue-specific vascular subpopulations.<sup>17</sup>

Notably, all of these cell types could be sensitive to radiotherapy. Endothelial cells have been reported to be one of the most radiosensitive among the fixed elements of mesenchyme.<sup>18</sup> In addition, applying radiotherapy to cancer patients could induce cellular senescence or cell death of the fibroblast population in normal tissues.<sup>19</sup> Furthermore, it was demonstrated that in radiotherapy patients, skin fibroblasts in noncancerous tissue have higher radiosensitivity and DNA damage than healthy ones.<sup>20</sup> Interestingly, MSCs have been proven to be comparatively radioresistant.<sup>21,22</sup> They are recruited to the injury sites, induce regional cell regrowth, and repair radiodermatitis.<sup>23</sup> Moreover, MSCs have been used in clinical trials for mitigating essential radiation injury in cancer patients.<sup>24–26</sup>

The radiation-induced bystander effect indicated changes in gene expression as one of the cells' significant responses. The genes responsible for apoptosis, angiogenesis, antioxidant activity, and irradiation sensitivity are the most susceptible during irradiation.<sup>27</sup> However, the alteration of the expression of these genes has not been widely elucidated in stromal cells.

Another concern is the limitation in the biocompatibility study of melanin NPs. There has been little evidence of its safety and bioactivity in normal cells. Most cytotoxicity evaluations of melanin NPs have been performed on commercial cancerous cell lines,<sup>28</sup> and the results are controversial. Some papers have shown that melanin supports the proliferation of murine embryonic stem cells<sup>29</sup> and PC12 cells.<sup>30</sup> Another study reported that melanin at high concentrations reduced the viability of NIH3T3 fibroblasts.<sup>31</sup> Remarkably, a recent study in 2021 indicated that noncancerous cells did not digest melanin NPs, while metastatic cells were massively absorbed.<sup>32</sup> In addition, metastatic cancer cells that highly take up melanin NPs are more cytotoxic and sensitive to radiation than nonmetastatic cells that do not take up melanin NPs.<sup>32</sup> These results led to a question as to whether the uptake of melanin NPs correlated with the biocompatibility and radioprotective activity of this compound in healthy cells as they did in cancer cells.

In this study, we aimed to evaluate the effects of squid ink melanin NPs on cell viability, cellular function, and expression of irradiation-susceptible genes in primary human fibroblasts (hFBs), human umbilical vein endothelial cells (hUVECs), and umbilical cord-derived mesenchymal stem cells (UCMSCs). More importantly, the protective ability of this NP against X-ray irradiation on these cells was also revealed in the cellular and molecular ranges. The safety of this compound was also demonstrated in a zebrafish embryo in an *in vivo* model.

## 2. METHODS

### 2.1. Production and Characterization of Melanin NPs.

Following a previous study, melanin was produced from squid ink sacs.<sup>8,9</sup> Melanin NPs were prepared by using sodium hydroxide (0.5 M/L). After that, hydrochloric acid solution was utilized to modify the pH of the melanin NP solution to 7.2. Melanin NPs were created at room temperature and atmospheric pressure. A Nanosem 450 scanning electron microscope was used to characterize the surface structure of melanin and melanin NPs. Fourier transform infrared (FTIR)

spectroscopy was applied to identify the chemical groups of melanin NPs (IRAffinity-1S, Shimadzu, Kyoto, Japan).

**2.2. Cell Culture.** hFBs were cultured in DMEM/F12 medium (Gibco, USA) supplemented with 10% fetal bovine serum (FBS, Gibco, USA), 100 units/mL penicillin, and 100  $\mu$ g/mL streptomycin (Gibco, USA). hUVECs were cultured in an EBM-2 medium kit (Lonza, Swiss). UCMSCs were grown on the culture flask surface coated with CELLstart CTS (CELLstart) in StemMACSTM MSC Expansion Media (StemMACS, Miltenyi Biotec). All hUVECs, hFBs, and UCMSCs were cultured at 37 °C with 5% CO<sub>2</sub>.

**2.3. Cell Viability Assay.** Cells were plated on 96-well plates at 2500 cells per well and incubated at 37 °C for 24 h in a humidified atmosphere with 5% CO<sub>2</sub>. Then, the wells were treated with melanin NPs at concentrations of 3.9, 7.8, 15.6, 31.3, 62.5, and 125  $\mu$ g/mL and continuously incubated for 24, 48, and 72 h. After that, 15  $\mu$ L of a dye solution of the MTT labeling reagent (final concentration 0.5 mg/mL) was added to each well. After incubation and solubilization, the absorbance of the cells was measured at 570 nm using an ELISA plate reader (BioTech Power Wave XS, Winooski, VT, USA). The experiments were performed in triplicate.

**2.4. X-ray Exposure.** Cells were cultured in six-well plates and either received melanin NP treatment at 25  $\mu$ g/mL (treated group) or not (control group) for 24 h. Cells were then exposed to X-ray radiation at 3, 5, 7, and 10 Gy doses with a single dose rate of 0.6 Gy/min using a Precise Digital Accelerator 152377 (ELEKTA, Stockholm, Sweden). Cells were continuously cultured for 48 h before being collected for downstream experiments.

**2.5. Quantitative RT-PCR.** Cells were seeded in six-well plates at 8000 cells/cm<sup>2</sup> per well. Cells were incubated with melanin NPs at 25  $\mu$ g/mL overnight before exposure to an X-ray irradiation dose from 0 to 5 Gy. Two days post radiation, the cells were harvested and subjected to RNA isolation using an RNA extraction kit (Thermo Scientific, Waltham, MA, USA). Then, the Revert Aid First Strand cDNA Synthesis Kit (Thermo Scientific, Singapore) was used to synthesize cDNA from total RNA. The transcript levels of genes encoding vascular endothelial growth factor A (VEGF-A), caspase-3, superoxide dismutase 1 (SOD1), and interleukin (IL)-1 $\alpha$  were determined by quantitative real-time polymerase chain reaction (RT-PCR) using a 7500 real-time PCR instrument (Applied Biosystems, CA).  $\beta$ -actin and glyceraldehyde-3-phosphate dehydrogenase (GAPDH) genes were used as housekeeping genes for the control. Primer sequences were either designed or referred from the literature<sup>33,36</sup> and are presented in Table 1.

**2.6. Wound Healing Assay.** Cells were cultured in suitable 24-well plates at 8000 cells/cm<sup>2</sup> density. When cells reached a density >95% of the culture plate, they were supplemented with mitomycin (10  $\mu$ g/mL) for 2 h to inhibit cell proliferation before wound creation using a scratcher (SLP, Korea). Afterward, the cells were supplemented with melanin NPs at 25, 50, and 75  $\mu$ g/mL. The process of wound healing was observed and captured by optical microscopy. Image results were analyzed by ImageJ software (version 1.46r).

**2.7. Senescence Cell Analysis.** The percentages of senescent cells in the hUVECs, hFBs, and UCMSCs were evaluated using the Senescence Cells Histochemical Staining Kit (Sigma–Aldrich, Missouri, USA).

Cells were seeded on six-well plates at 20,000 cells/cm<sup>2</sup> density and incubated with melanin NPs at concentrations of

**Table 1. Primers**

primer	sequences (5'-3')
human- $\beta$ -actin-F	GAG TAC AGA GCC TCG CCT AT
human- $\beta$ -actin-R	TTA AGC CGG CCT TGC ACA TG
human-caspase 3-F	AGG CCG ACT TCT TGT ATG CA
human-caspase 3-R	TTC TGT TGC CAC CTT TCG GT
human-SOD-F	ACA AAG ATG GTG TGG CCG AT
human-SOD-R	AAC GAC TTC CAG CGT TTC CT
human-VEGFA-R	AGGAGGAGGGCAGAATCATCAC
human- VEGFA-R	ATGTCCACCAGGGTCTCGATTG
human-IL1a-F	AAG ATG GCC AAA GTT CCA GAC A
human-IL1a-R	TCC TTG AAG GTA AGC TTG GAT G
human-GAPDH-F	GGTGTGAACCATGAGAAGTATGA

50 or 25  $\mu\text{g}/\text{mL}$  at 37 °C and 5%  $\text{CO}_2$  for 48 h. Then, the culture medium was removed, and the cells were washed with phosphate-buffered saline (PBS) before being fixed with 1X fixation buffer for 7 min. Cells were washed twice with 1X PBS and incubated with a staining mixture overnight at 37 °C and 5%  $\text{CO}_2$ . Cells were stained with DAPI staining solution (Abcam, Cambridge, UK) for 15 min after removal of the staining mix and washed once with PBS. Cells were washed once with PBS and observed and captured under optical and fluorescence microscopes (Olympus, Tokyo, Japan). Images were analyzed with ImageJ software (version 1.46r).

**2.8. Angiogenesis Assay.** Cells were cultured in EBM-2 medium until reaching 80% confluency and then collected for the angiogenesis experiment using an angiogenesis assay kit (Abcam, UK) following the manufacturer's protocol. Cells were seeded into six-well plates at a density of  $20 \times 10^4$  cells/well, and all wells were coated with an extracellular matrix solution. Experimental cell wells were treated with melanin NPs at 50 and 25  $\mu\text{g}/\text{mL}$  in hUVECs and 25  $\mu\text{g}/\text{mL}$  in hFBs and UCMSCs. Suramin (50  $\mu\text{g}/\text{mL}$ ) was added to the negative control wells.

Irradiation was performed after cells were seeded on a six-well plate, and melanin NPs were added at 25  $\mu\text{g}/\text{mL}$ . Cells were then exposed to X-rays at different dosages (0 Gy, 3 Gy, 7 Gy) and grown for 10 h at 37 °C and 5%  $\text{CO}_2$ . Angiogenesis processes in the wells were observed and captured by fluorescence microscopy at 490/540 nm. Images were analyzed using ImageJ software (version 1.46r).

**2.9. Multilineage Differentiation.** The trilineage differentiation capacity of UCMSCs for osteogenesis, adipogenesis, and chondrogenesis was tested with the StemPro Osteogenesis Differentiation Kit, StemPro Adipogenesis Differentiation Kit, and StemPro Chondrogenesis Differentiation Kit (Gibco, USA), respectively. To test the protection ability of melanin NPs, irradiation was performed after the cells were seeded on a culture plate and melanin NPs were added at a concentration of 25  $\mu\text{g}/\text{mL}$ . Cells were then exposed to X-rays at a dose of 3 Gy. Differentiated cells were confirmed by Alizarin Red staining (osteogenesis), Oil Red O staining (adipogenesis), and Alcian Blue staining (chondrogenesis). All staining solutions were supplied with the kits. StemMACS MSC Expansion Media was used as an undifferentiated control. Cells were cultured in differentiation media for 14 days before being fixed with 4% paraformaldehyde (Sigma-Aldrich) and stained as described above.

**2.10. In Vivo Zebrafish Embryonic Toxicity Assays.** A zebrafish embryotoxicity assay was performed as per the OECD Test 236.<sup>37</sup> Briefly, healthy 2-hpf (hours post

fertilization) embryos were individually placed into 24-well microplates containing melanin NPs diluted in E3 medium (5 mM NaCl, 0.17 mM KCl, 0.4 mM  $\text{CaCl}_2$ , and 0.16 mM  $\text{MgSO}_4$ ) and incubated at 26 °C. After the range-finding test, the following concentrations were selected: 0 (control), 10, 50, 100, 200, 300, and 500 mg/L. The embryonic mortality and morphology were monitored daily to calculate the LC50 (lethal concentration 50), EC50 (half maximal effective concentration 50), and TI (teratogenic indices) values. The dead embryos were removed, and the solutions were refreshed to 96 hpf. To investigate the interaction between melanin NPs and X-rays on living organisms, a concentration of 25 mg/L was selected for the study. Zebrafish embryos were exposed to 25 mg/L melanin NPs starting at 2 hpf, with daily renewal until 96 hpf, and X-ray irradiation was performed at 24 hpf. All four groups' lethal and morphological data (with/without melanin NPs and with/without X-rays) were recorded.

**2.10.1. ROS Assay.** The cells were seeded on the 96-well plate at 5000 cells/ $\text{cm}^2$  density in DMEM/F12 plus 5% FBS at 37 °C and 5%  $\text{CO}_2$  for 8 h to let the cells attach on the culture surface. The medium was removed, and then fresh medium was added with or without nanomelanin at 50  $\mu\text{g}/\text{mL}$ . After 24 h of incubation, the cells were washed with PBS. ROS inducer was added into the corresponding wells. Then, 25  $\mu\text{M}$  H2DCFDA was added and incubated for 30 min at 37 °C. Cells were washed with PBS, and the optical density was measured using SpectraMax M3 (Molecular Devices, USA) at 529 nm.

**2.11. Statistical Analysis.** In this study, all experiments were repeated three times, and the data collected were statistically analyzed using the required techniques. Student's *t* test and ANOVA were used for comparisons between groups. A *p* value <0.05 was used to determine a significant difference.

### 3. RESULTS

#### 3.1. Production and Characterization of Melanin NPs.

Melanin is a natural pigment with a polymer structure found in a greater number of living organisms. Scanning electron microscopy (SEM) was used to capture the structures of melanin and melanin NPs at 30,000 $\times$  and 50,000 $\times$  magnifications, respectively (Figure 1A,B). The SEM image at 30,000 magnifications showed the surface structure of both melanin and melanin NPs. In Figure 1A, the subnanostructures with oval shapes were interlaced to create the rough surface of the material. Furthermore, the structure of the melanin NPs after breaking the polymer at the nanoscale was revealed by SEM images (Figure 1B). In addition, the functional groups of melanin NPs, such as the hydroxyl (–OH) and carbonyl (–CO–) groups, were detected in the FTIR spectra (Figure 1C). The spectrum peaks were scanned from 399 to 4000  $\text{cm}^{-1}$  at a resolution of 4  $\text{cm}^{-1}$ . The zeta potential is one of the easily measurable properties of the stability of colloidal dispersions of NPs. The zeta potential value reflects the degree of electrostatic attraction between neighboring NPs. The smaller the zeta potential value, the better the dispersion of the particles in solution and the less tendency they have to coagulate. These melanin NPs had a zeta value of  $-9.3 \pm 2.6$  (Figure 1D).

**3.2. Melanin Was Insoluble and Had Low Cytotoxicity.** After being added to the cell culture, melanin stayed in large clumps in the cell culture medium, as shown in Figure 2A. The higher the doses, the bigger the aggregations were observed. These aggregations were easy to be washed away. At

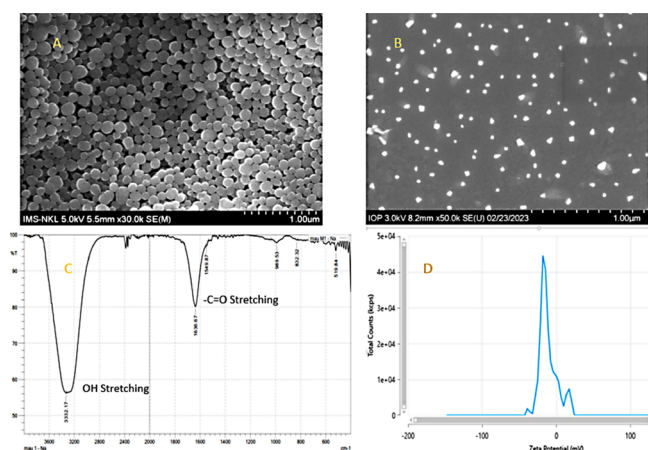


**Figure 1.** Synthesis of melanin NPs from the extracted melanin of a squid ink. (A) Extracted melanin under SEM at a magnification of 30,000 $\times$ . (B) Melanin NPs under SEM at a magnification of 50,000 $\times$ . (C) FTIR spectra of melanin NPs. (D) Zeta potential of melanin NPs.

concentrations ranging from 7.8 to 125  $\mu\text{g}/\text{mL}$ , melanin was less cytotoxic to the tested cells (Figure 2B). The IC<sub>50</sub> values were not determined in either hFBs or UCMSCs as cell viability was maintained higher than 70% at all tested concentrations (Figure 2B). These data indicated the low cytotoxicity of melanin but confirmed the insolubility of this compound.

**3.3. Melanin NPs Had Low Cytotoxicity and No Effect on Cell Senescence.** At concentrations ranging from 3.9 to 125  $\mu\text{g}/\text{mL}$ , melanin NPs were less cytotoxic to all three tested cell types (Figure 3A). The IC<sub>50</sub> values were not determined in hUVECs as cell viability could not reach below 50% at all test concentrations. In hFBs, the IC<sub>50</sub>72h value was  $119.7 \pm 3.2 \mu\text{g}/\text{mL}$ . In addition, these NPs had the most cytotoxic

effect on UCMSCs, with an IC<sub>50</sub>72h value of  $74.1 \pm 2.4 \mu\text{g}/\text{mL}$  (Table 2).

The morphology of cell nuclei was also checked in the presence of melanin NPs at 50  $\mu\text{g}/\text{mL}$  after 72h of incubation, showing the similarity in their size and shape between the treated and control cell nuclei (Figure 3B). For cellular senescence induction, in the presence of melanin NPs (25 and 50  $\mu\text{g}/\text{mL}$ ), few  $\beta$ -galactosidase<sup>+</sup> cells were observed in hFB and UCMSC populations. Among the three cell types, hUVECs had the highest percentage of senescent cells ( $6.2 \pm 0.20\%$ ) compared to hFBs ( $0.3 \pm 0.09\%$ ) and UCMSCs ( $0.5 \pm 0.05\%$ ) ( $p < 0.001$ ) (Figure 3C). Quantitative analysis showed that the rates of cellular senescence were not significantly different between the control and treated groups (all  $p$  values  $>0.05$ ) in all three cell lines (Figure 3D). These data demonstrated that melanin NPs did not affect the cellular senescence in hFBs, hUVECs, or UCMSCs.

**3.4. Melanin NPs Maintained the Multilineage Differentiation Capacity of Irradiated UCMSCs.** Multilineage differentiation is a major functional characteristic of UCMSCs. Therefore, we first checked whether melanin NPs could affect this function of stem cells. The results showed that in the presence of melanin NPs (25  $\mu\text{g}/\text{mL}$ ), UCMSCs still differentiated into osteoblasts, chondrocytes, and adipocytes (Figure 3E). In the meantime, X-ray irradiation disturbed the differentiations. It caused a reduction in the color of Alizarin Blue and prevented cell aggregation into the cartilage-like structure in the chondrogenesis assay. Irradiation also decreased the number of lipid-rich vacuoles in adipogenic-induced cells. However, osteogenesis was not affected by irradiation at 3 Gy. In the presence of melanin NPs, irradiated UCMSCs formed cartilage-like structures during chondrogenic induction, forming more lipid-rich vacuoles during adipogenesis (Figure 3E). These results indicated that melanin NPs expressed a protective ability by recovering chondrogenesis and adipogenesis in irradiated stem cells.

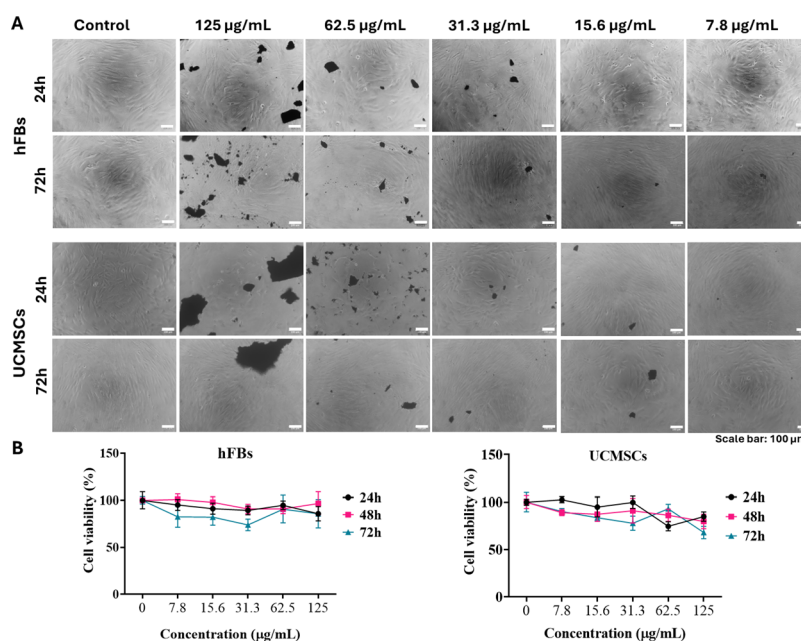


**Figure 2.** In vitro cytotoxicity of melanin on hFBs, and UCMSCs. (A) Images of cell culture in the presence of melanin powder at different concentrations. (B) Percentage of viable cells in the presence of melanin at concentrations ranging from 0 to 125  $\mu\text{g}/\text{mL}$  after 24, 48, and 72 h of incubation.

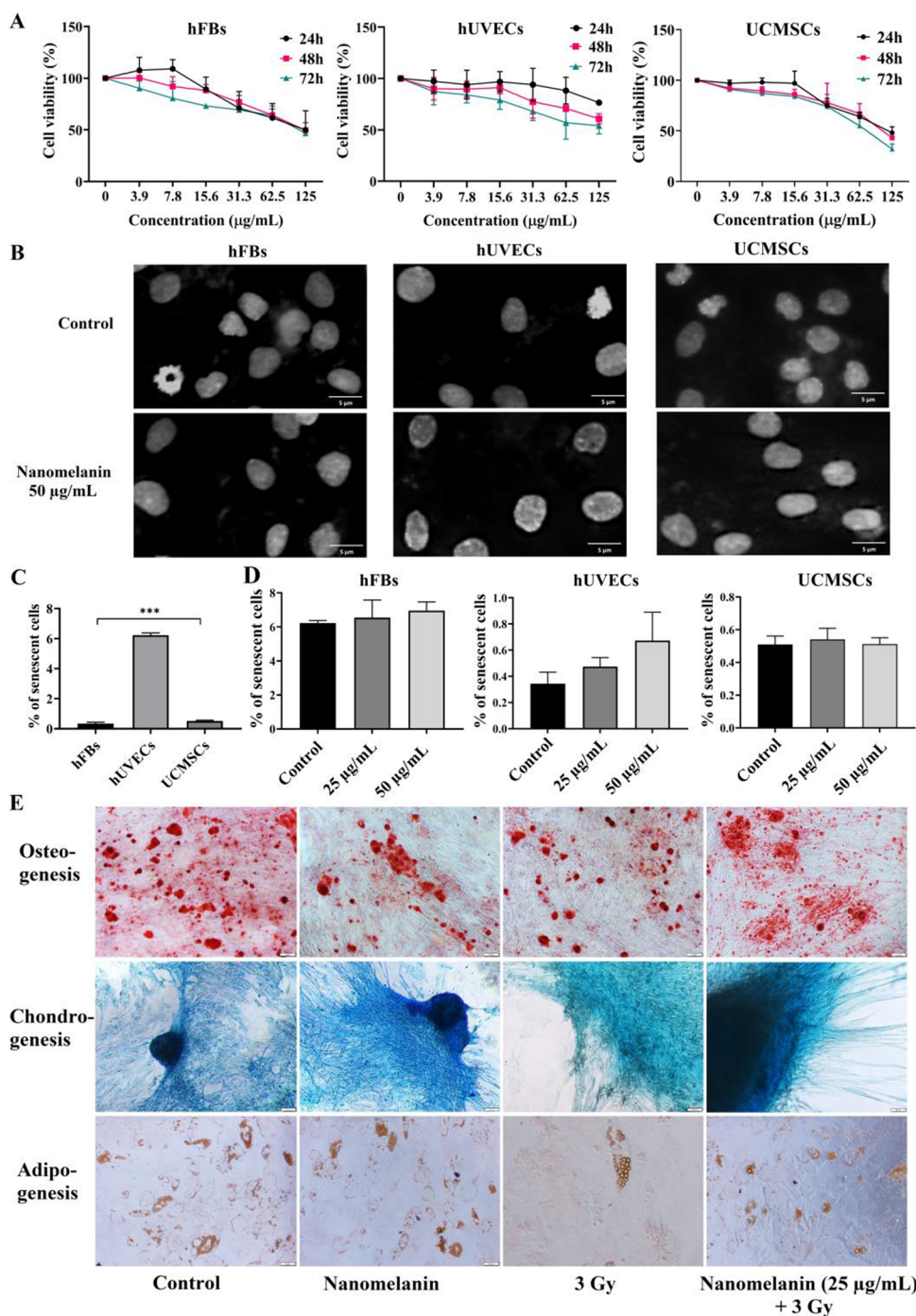


**Figure 3.** In vitro biocompatibility of melanin NPs on hUVECs, hFBs, and UCMSCs. (A) Percentage of viable cells in the presence of melanin NPs at concentrations ranging from 0 to 125  $\mu\text{g}/\text{mL}$  after 24, 48, and 72 h of incubation. (B) Morphology of cell nuclei in the presence of NPs at 50  $\mu\text{g}/\text{mL}$  after 72 h of incubation. (C) Senescence rates (%) in three cell types. (D) Effect of melanin NPs on cell senescence in hFBs, hUVECs, and UCMSCs. (E) Effect of melanin NPs on the cell differentiation of UCMSCs. Data are presented as the mean  $\pm$  SD,  $n = 3$ ,  $***p < 0.001$ .

**Table 2.** IC50 Values ( $\mu\text{g}/\text{mL}$ ) of Melanin NPs on hFBs, hUVECs, and UCMSCs<sup>a</sup>

	24 h	48 h	72 h
hFBs	ND	121.4 $\pm$ 7.2	119.7 $\pm$ 3.2
hUVECs	ND	ND	ND
UCMSCs	114.8 $\pm$ 5.1	106.8 $\pm$ 0.5	74.1 $\pm$ 2.4

<sup>a</sup>ND: not determined.

### 3.5. Melanin NPs Prevented Cell Migration in hUVECs and UCMSCs But Not in hFBs.

We performed a wound-healing assay to determine whether melanin NPs affect cell migration (Figure 4A). After 72 h of treatment, the wound closure of the control group in hFBs, hUVECs, and UCMSCs reached 97.5  $\pm$  2.9, 99.8  $\pm$  0.2, and 92  $\pm$  0.7%, respectively (Figure 4B). In hFBs, none of the three doses of melanin NPs inhibited cell migration after 72 h of incubation ( $p > 0.05$ ). In hUVECs, at all time points, the rate of cell migration after

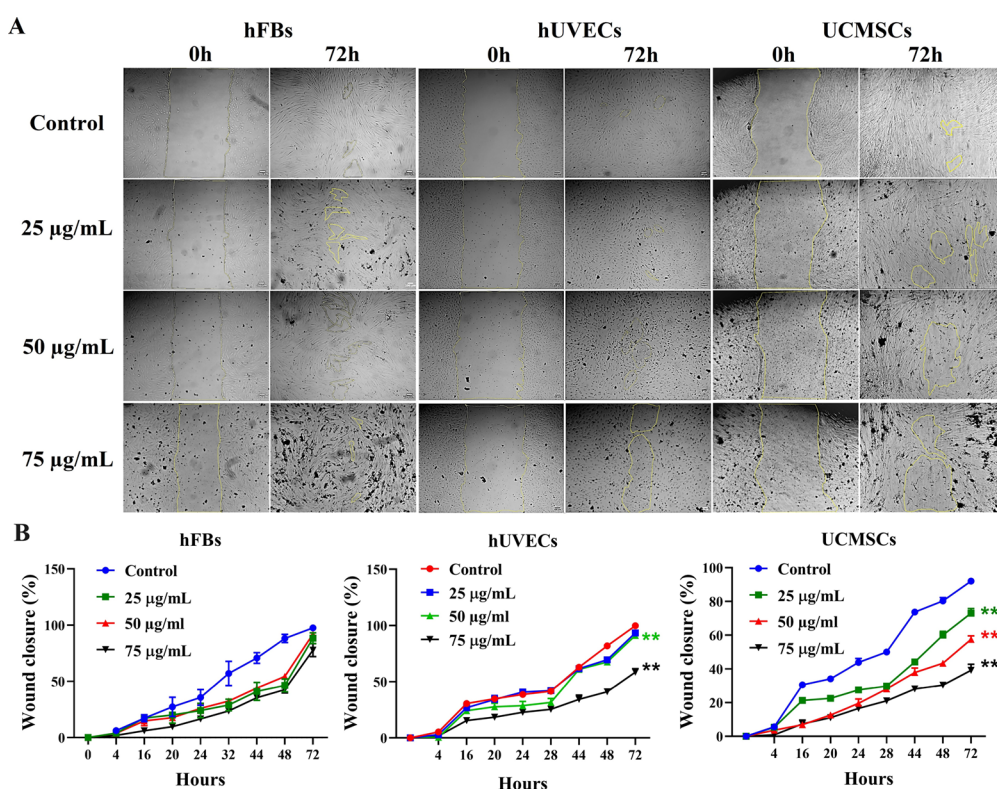


**Figure 4.** Effect of melanin NPs on the migration of hFBs, hUVECs, and UCMSCs. (A) Images of the wounded site on the monolayer culture of cells incubated with nanomelanin at different doses and times. (B) Quantitative wound closure rates in hFBs, hUVECs, and UCMSCs were recorded every 4 h up to 72 h of measurement. Data were repeated in triplicate and presented as the mean  $\pm$  SD,  $n = 3$ .  $**p < 0.01$  vs control. Scale bar: 100  $\mu$ m.

treatment with melanin NPs at 25  $\mu$ g/mL was not significantly different from that of the control ( $p > 0.05$ ).

However, it markedly decreased at concentrations of 50 and 75  $\mu$ g/mL after 72 h of incubation ( $p < 0.01$ ) (Figure 4B). The most potent inhibitory effect was observed in UCMSCs ( $p < 0.001$ ), with the percentage of wound closure at 75  $\mu$ g/mL after 72 h being  $39.2 \pm 3.6\%$ , corresponding to 42.6% of the control (Figure 4B). These results demonstrated that melanin NPs could selectively prevent cell migration in hUVECs, especially in UCMSCs.

**3.6. Melanin NPs Penetrated Efficiently hUVECs But Less in hFBs or UCMSCs.** During the wound-healing assay, we observed different distributions of melanin NPs in different cell types. Hence, we analyzed the penetration ability of this substance at a dose of 75  $\mu$ g/mL after 72 h of incubation. As shown in Figure 5A, the NPs were well localized inside the hUVECs and concentrated in the cytoplasm surrounding the cell nuclei (indicated as red arrows). Meanwhile, melanin NPs tended to stay as clusters outside hFBs, especially of UCMSCs (marked with red circles). It is worth noting that all three cell types were treated with the same amount of melanin NPs, with good dispersion at the beginning of the incubation (Figure 5A). After addition to the cell culture medium, the NPs quickly aggregated in hFBs and UCMSCs, forming large clusters in the culture wells; meanwhile, a small number of NP clusters was present in the hUVEC culture. Next, we focused on analyzing NP penetration in hUVECs at different doses and times. The NPs concentrated in the cytoplasm in a dose-dependent manner and over time (Figure 5B). The more time and higher doses there were, the more NPs were inside the cells. These

data indicate that hUVECs more efficiently took up melanin NPs than hFBs and UCMSCs.

**3.7. Melanin NPs and Irradiation Synergistically Inhibited Tube Formation in hUVECs.** The results obtained above expressed the different effects of the melanin NPs in hUVECs. Therefore, we continued to check the impact of this substance on the in vitro tube formation capacity of this cell type. The results showed that melanin NPs suppressed the angiogenesis process in a dose-dependent manner in hUVECs (Figure 6A). At the 50  $\mu$ g/mL concentration, the NPs significantly reduced the total tube length, branching, and segments by 2.1 times ( $p < 0.01$ ), 2.8 times ( $p < 0.001$ ), and 3.7 times ( $p < 0.001$ ), respectively (Figure 6B). Meanwhile, at the 25  $\mu$ g/mL concentration, melanin NPs did not affect the total tube length ( $p > 0.05$ ). Still, they reduced the total tube branching and a segment approximately 1.2 times ( $p < 0.05$ ) (Figure 6B). At 25  $\mu$ g/mL nanomelanin, we checked whether melanin NPs could rescue the angiogenesis process in this cell type under irradiation conditions. The data showed that X-rays completely inhibited the tube formation of hUVECs at 3 and 7 Gy. In addition, in the presence of melanin NPs at a 25  $\mu$ g/mL concentration, the irradiated cells could not make the capillary-like tubular structure as the control (Figure 6C). These results demonstrated that melanin NPs did not show radioactive protection ability toward angiogenesis in hUVECs.

**3.8. Melanin NPs Recovered the Expression of Functional Genes in hFBs But Not in hUVECs Under Irradiation.** The negative impact of melanin NPs on the function of hUVECs prompted us to check the effect of this substance on stromal cells at the molecular level. The radioprotective role of this NP was also investigated. The

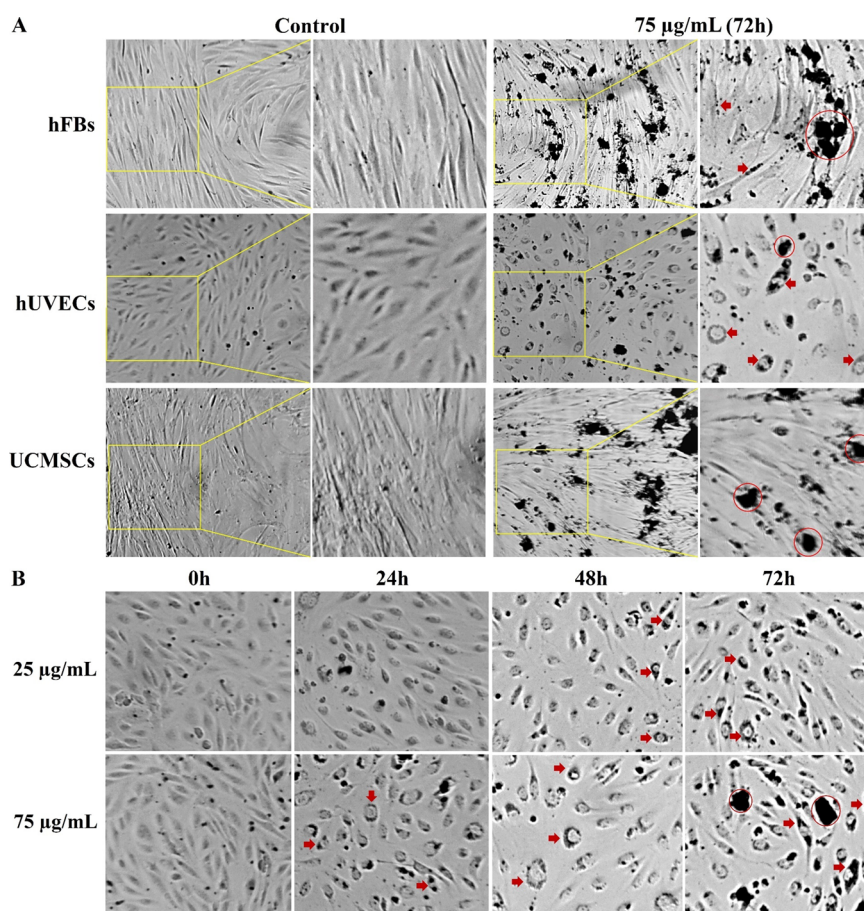


**Figure 5.** Penetration of melanin NPs in hFBs, hUVECs, and UCMSCs. (A) Presence of melanin NPs in the cell population at a dose of 75 µg/mL after 72 h of incubation. (B) Uptake of melanin NPs in hUVECs at two doses of 25 and 75 µg/mL at 24, 48, and 72 h of incubation.

effect of melanin NPs (25 µg/mL) and irradiation (at 3 Gy) on the expression of functional genes was determined for the angiogenesis gene VEGF-A, apoptotic gene Caspase-3, antioxidant gene SOD, and irradiation sensitivity gene IL-1 $\alpha$ . Regarding hFBs, melanin NPs showed no effect on the expression of this gene ( $p > 0.05$ ). Meanwhile, irradiation significantly reduced the expression of VEGF-A by 1.9 times at 3 Gy ( $p < 0.0001$ ). Interestingly, in melanin NP-subjected cells, there was a significantly increased expression of VEGF-A ( $p < 0.05$ ) after irradiation, even though it was still not equal to the control ( $p < 0.05$ ). For apoptosis, irradiation and melanin NPs did not affect the expression of Caspase 3 ( $p > 0.05$ ). For the antioxidant gene, irradiation reduced the expression of SOD, but melanin NPs protected the expression of this gene, although not significantly ( $p > 0.05$ ). Similarly, X-ray radiation induced the expression of IL-1 $\alpha$  ( $p < 0.0001$ ). Still, in the presence of melanin NPs, the expression of this gene remarkably stabilized to the level of the control ( $p > 0.05$ ) (Figure 7A).

In hUVECs, radiation and melanin NPs strongly inhibited the expression of VEGF-A ( $p < 0.01$ ). Melanin NPs and irradiation synergistically reduced the gene expression level by 4 times at 3 Gy compared to irradiation alone ( $p < 0.05$ ). For the other genes, irradiation significantly reduced their expression ( $p < 0.0001$ ); meanwhile, melanin NPs also decreased their expression, but only significantly for the SOD gene ( $p < 0.01$ ). Remarkably, melanin NPs did not exert

protective activity for these genes under X-ray exposure (Figure 7B).

Notably, in UCMSCs, the expression of the tested genes was insignificantly altered under radiation conditions ( $p > 0.05$ ), except for IL-1 $\alpha$  ( $p < 0.05$ ). Similarly, melanin NPs did not impact most tested genes but inhibited the expression of VEGF-A ( $p < 0.05$ ). Remarkably, melanin NPs tended to stabilize the expression of IL-1 $\alpha$  under irradiation ( $p < 0.05$ ) (Figure 7C).

The obtained data demonstrated that in hFBs, melanin NPs tended to protect the expression of functional genes to normal levels after X-ray exposure. In hUVECs, melanin NPs altered the gene expression; moreover, under irradiation conditions, melanin NPs did not show a protective ability. In contrast, irradiation and melanin NPs did not significantly impact these genes in UCMSCs (Figure 7D).

**3.9. Melanin NPs Protected Cell Viability against Irradiation in hFBs But Not in hUVECs.** Irradiation at doses ranging from 3 to 10 Gy differentially affected the viability of the three tested cell types. After irradiation, we observed a substantial reduction in the cell density of hFBs and hUVECs but not UCMSCs (Figure 8A). A marked effect was observed in hFBs; at doses of 3, 5, 7, and 10 Gy, the percentages of cell viability in this cell type sharply decreased to 33, 31, 19, and 1% (of the control), respectively. Regarding hUVECs, these values were 56, 47, 26, and 2% (of the control), respectively. Interestingly, the impact of irradiation was significantly lower in UCMSCs (Figure 8B). The viability of UCMSCs under

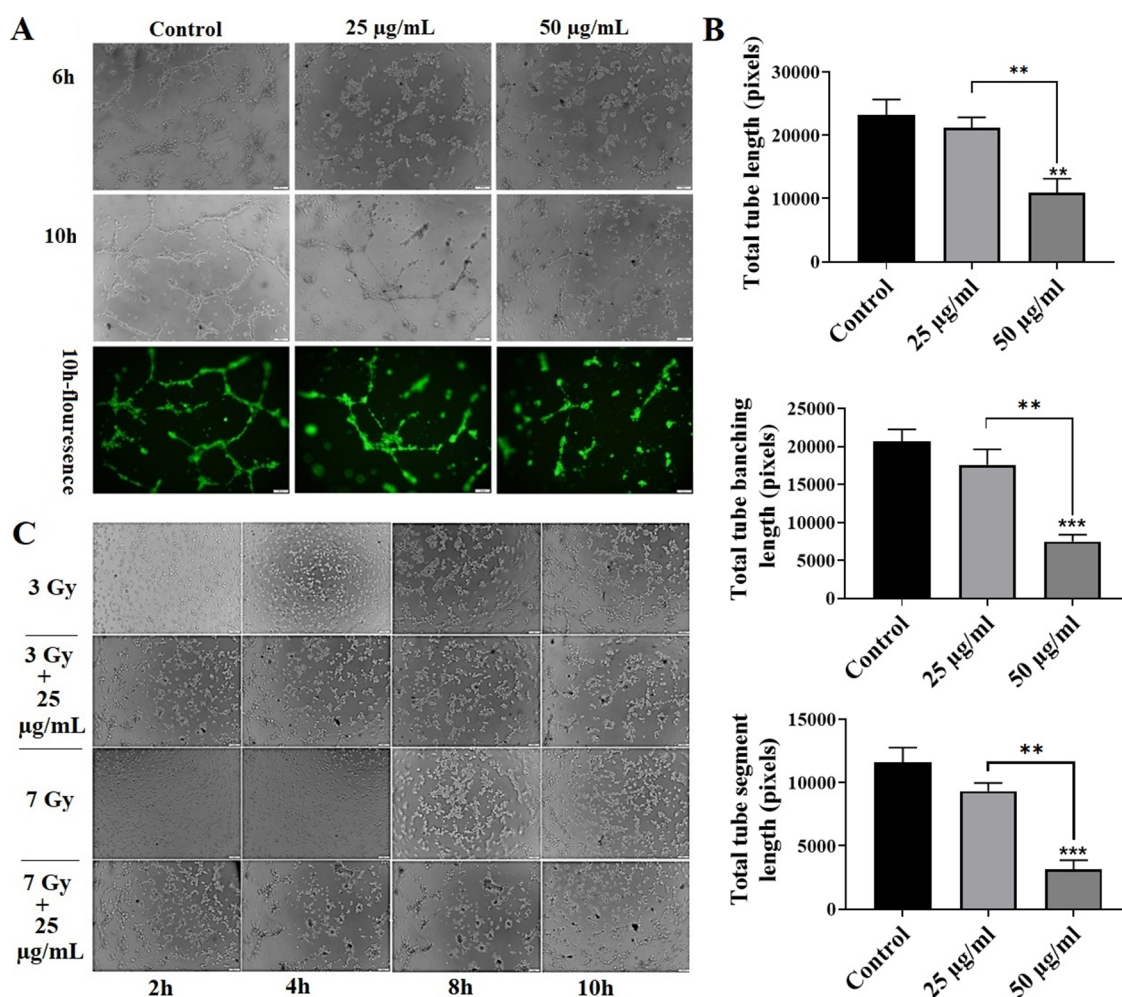


**Figure 6.** Effects of melanin NPs on the tube formation of hUVECs. (A) Tube formation in hUVECs in the presence of nanomelanin at two doses: 25 µg/mL and 50 µg/mL. (B) Quantification of tube formation in hUVECs. (C) Effect of nanomelanin on tube formation in hUVECs exposed to X-rays at two doses of 3 and 7 Gy, with or without nanomelanin at 25 µg/mL. Data are presented as the mean  $\pm$  SD,  $n = 3$ . \*\* $p < 0.01$ ; \*\*\* $p < 0.001$ . Scale bar: 100 µm.

radiation at 3 and 5 Gy was 86.7 and 81.9%, respectively ( $p < 0.01$ ). Even at higher doses (7 and 10 Gy), the percentages of cell viability were 65.3 and 63.2%, respectively, much higher than those observed in hFBs and hUVECs ( $p < 0.001$ ) (Figure 8B). These data indicated that irradiation selectively influenced cell types and that UCMSCs expressed irradiation resistance.

Remarkably, melanin NPs successfully restored cell viability in hFBs. The cell density increased in this cell population. At the same time, no such observation was made in hUVECs (Figure 8A). At doses of 3, 5, and 7 Gy, the viability of hFBs was 86, 78, and 65% corresponding to recovery rates of 2.6, 2.5, and 3.4 times, respectively. However, in the presence of melanin NPs, the cell viability of the hUVECs did not recover but was rather slightly decreased. In UCMSCs, the percentages of cell viability at higher irradiated doses (7 and 10 Gy) increased but not significantly compared to the control ( $p > 0.05$ ) (Figure 8B).

Besides, the ROS assay indicated that nanomelanin could significantly scavenge the amount of free radicals after ROS induction in hFBs (Figure 8C).

These results proved that melanin NPs could selectively protect certain cell types from radiation.

**3.10. Melanin NPs Were Not Toxic to Zebrafish Embryonic Development.** The *in vivo* toxicity of melanin

NPs was demonstrated in the development of zebrafish larvae. The visible defect was observed only at doses of 200 mg/L and higher (Figure 9A). The toxicity effect with an LC50<sub>96h</sub> of 205 mg/L, higher than the GHS' 100 mg/L threshold, indicated the nonaquatotoxic nature of the compound.<sup>37,38</sup> The EC50<sub>96h</sub> was 204 mg/L (Figure 9B), leading to a TI value of  $< 1$ , which means that the compound was a nonteratogenic drug.<sup>37,38</sup>

Since doses below 50 mg/L exert no effect on the survival rate and morphology, we selected a concentration of 25 mg/L (corresponding to 25 µg/mL) for the irradiation experiments, similar to that used with the cells. No lethality or morphological defects were observed in any condition (with/without melanin NPs and all irradiation doses) (Figure 9C), suggesting that at the body level, melanin NPs do not synergistically interact with X-rays in terms of damaging the organism.

#### 4. DISCUSSION

The synthesis of nanosized melanin poses many challenges because the final product frequently differs from natural melanin due to changes in its structural and functional features.<sup>4,28</sup> There are very few studies on the biocompatibility of melanin NPs in the literature. In addition, the impact of melanin NPs on cell proliferation has been controversially



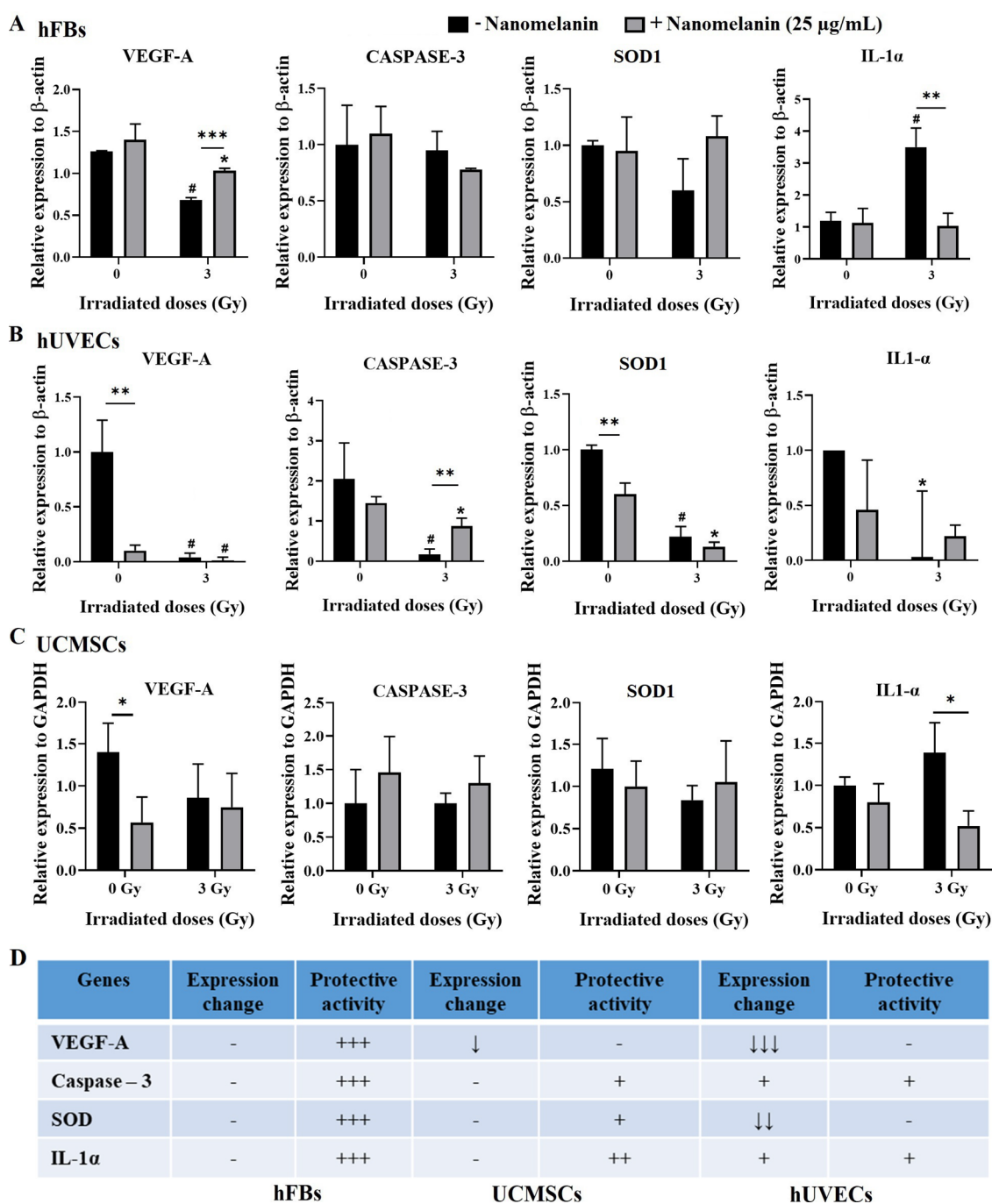


**Figure 7.** Effect of irradiation and nanomelanin on the expression of functional genes. (A) Expression of tested genes in hFBs under treatment conditions of nanomelanin and radiation. (B) Expression of tested genes in hUVECs under nanomelanin and radiation treatment conditions. (C) Expression of tested genes in UCMSCs under treatment conditions of nanomelanin and radiation. (D) Summarization of the effects of melanin NPs on the expression of functional genes. Data are presented as the mean  $\pm$  SD,  $n = 3$ ,  $*p < 0.05$ ,  $**p < 0.01$ ,  $***p < 0.001$ ,  $\#p < 0.0001$ .

reported,<sup>28,31,32</sup> raising the necessity of testing the safety of this compound.

This study investigated the biocompatibility and radio-protective activity of melanin NPs on three primary cell lines: hUVECs, hFBs, and UCMSCs. It is worth noting that most of the reported papers evaluate the cytotoxicity of melanin and its nanoform on commercial cancerous cell lines, which are modified to adapt to the in vitro cell culture condition,<sup>29,30,32</sup> which may not reflect the accurate reaction of normal cells as the primary cells do.

Determination of cytotoxicity is the initial assessment of any medical material.<sup>39</sup> In the present study, the NPs had a low cytotoxicity on hFBs, hUVECs, and UCMSCs at 72 h of incubation. The compound did not induce the apoptosis gene Caspase-3 in any of the three cell types at 25  $\mu\text{g/mL}$ . In addition, cellular senescence was not elevated when treated with melanin NPs. This is crucial since these cells are the key players in regeneration.<sup>15–17</sup> If cellular senescence is induced, the cells will have irreversible proliferative withdrawal.<sup>40–42</sup> Moreover, melanin NPs did not alter the multilineage differentiation capacity of UCMSCs, one of the most

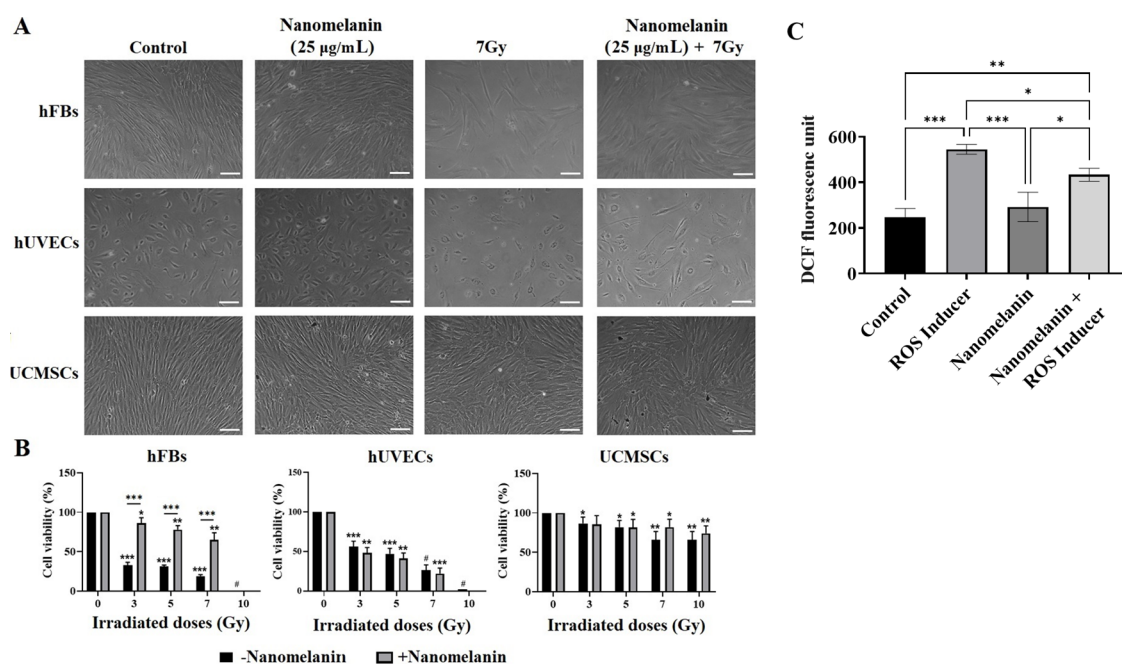


**Figure 8.** Protective effect of nanomelanin against irradiation on cell viability. (A) Changes in the morphology and density of cells associated with irradiation with or without nanomelanin. (B) Cell viability of hFBs, hUVECs, and UCMSCs was significantly recovered in the presence of nanomelanin at different irradiation doses. (C) Scavenging ROS of nanomelanin in the ROS assay. DCF: Dichlorofluorescein. Data are presented as the means  $\pm$  SDs,  $n = 3$ , \* $p < 0.05$ , \*\* $p < 0.01$ , \*\*\* $p < 0.001$ , # $p < 0.0001$ . Scale bar: 100  $\mu\text{m}$ .

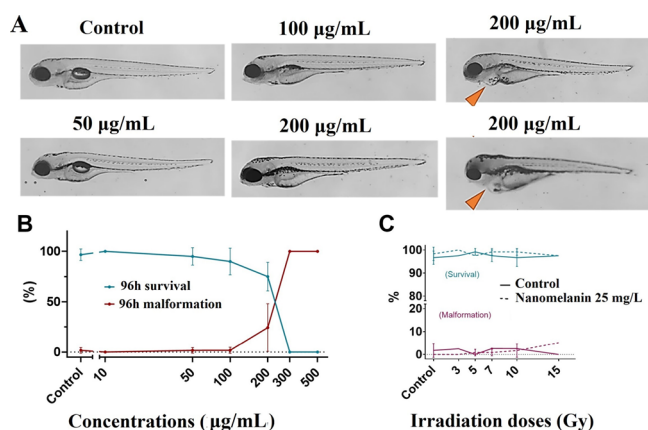


**Figure 9.** Nanomelanin exposure was safe for zebrafish embryo development. (A) Visible morphological defect was observed only at a dose as high as 200 mg/L, with heart edema being the main phenotype. (B) Dose–response curves of lethal and morphological effects. (C) Nanomelanin at 25 mg/L and irradiation until 15 Gy did not affect zebrafish embryonic development.

important characteristics of stem cells.<sup>14,15</sup> In addition, cell migration was partially inhibited by melanin NPs in UCMSCs and hUVECs but not in hFBs. In addition, we stained the cells treated with nanomelanin with Hoechst, a DNA fluorescence dye. The results showed that the morphology and size of the cell nuclei were maintained as the untreated one, indicating that nanomelanin did not cause a gross change in the cell nuclei. More specific analysis should be used for DNA damage in further works.

Remarkably, *in vitro* angiogenesis was suppressed in hUVECs in the presence of melanin NPs. The reduction in the expression of VEGF-A could mainly be causing this effect. Previous papers identified that VEGF-A is responsible for both cell migration and tube formation in endothelial cells.<sup>34,35</sup> In

the present study, the qRT-PCR assay showed that in both hUVECs and UCMSCs, the mRNA level of this gene significantly decreased in the presence of melanin NPs compared with the control; meanwhile, there was no change in the expression of VEGF-A in hFBs. The VEGF-A level was extremely reduced in hUVECs (10 times) compared with the control. Several previous studies pointed out the relationship between melanocyte pigmentation and VEGF-A. For example, the depression of melanin production was correlated with preventing VEGF receptor activity in melanocytes.<sup>33,36,43</sup> Most recently, Han et al. clarified that M2 macrophages stimulate melanocytes to produce melanin through the VEGF pathway.<sup>44</sup> Notably, our study is the first to report the direct effect of melanin NPs on the expression of VEGF-A in endothelial cells, consequently inhibiting angiogenesis *in vitro*. In addition, the NPs reduced the antioxidant gene SOD1 in hUVECs but not in hFBs and UCMSCs.

These data demonstrated that melanin NPs were selectively biocompatible with stromal cells, especially fibroblasts. However, the NPs selectively perturbed the function of endothelial cells at both the cellular and gene expression levels. The reason for the different impacts of melanin NPs on the three cell types may be due to their cellular internalization capacity. hUVECs showed the highest NP uptake ability compared with hFBs and UCMSCs. As reported in the literature, endothelial cells are amateur phagocytes that can clear various objects from the blood.<sup>45</sup> Fibroblasts and MSCs are limited in the phagocytosis of only apoptotic bodies.<sup>46,47</sup> Another reason for the higher internalization capacity in hUVECs compared to that in the two remaining cell types is the aggregation of the NPs when added to the culture medium. The formation of NP clusters in hFB and UCMSC cultures could prevent the penetration/uptake of the NPs. Which elements in the conditioned medium caused such accumulation should be elucidated. Nonetheless, our results revealed

that, similar to cancer cells, as reported,<sup>32</sup> the uptake of melanin NPs would affect the biocompatibility of cells.

The radioprotective activity of melanin NPs was identified when three cell types were irradiated at different doses. As observed in previous studies, the percentage of cell viability sharply decreased in both hFBs and hUVECs.<sup>18–22</sup> Fibroblasts showed more sensitivity to endothelial cells, consistent with previously published papers.<sup>41,48</sup> Interestingly, cell viability was recovered at every tested dose in the fibroblast population in the presence of NPs. This means that melanin in the form of NPs in this study maintained its ability to rescue cell survival from radiation. The ROS assay confirmed this protective effect, which showed the ROS scavenging ability of nanomelanin. This result strongly indicated that melanin NPs are a radiation-protective agent.

Moreover, the protective capacity of NPs was also observed at the molecular level in the hFBs. In the presence of melanin, the expression of the angiogenesis gene VEGF-A, the antioxidant gene SOD, and the irradiation sensitivity gene IL-1 $\alpha$  tended to return to normal levels after irradiation. Protecting gene expression meant that the irradiated cells could be healed from the damage caused by radiation.<sup>49–51</sup>

However, the radiation-protective effect of melanin NPs was not observed in hUVECs. This substance could not restore cell viability following irradiation. In addition, the NPs and irradiation synergistically inhibited tube formation in hUVECs. Moreover, melanin NPs in irradiated hUVECs synergistically induced apoptosis genes and reduced the number of antioxidant genes. Once again, the results demonstrated that melanin NPs selectively protected hFBs but not hUVECs from radiation. As indicated in previous papers, melanin NPs could be applied in cancer therapy.<sup>4,9</sup> In our current study, the effect of melanin NPs on endothelial cells has excellent implications for cancer treatment. The anticancer effects of melanin and melanin NPs have been reported based on their antioxidant and anti-inflammatory activities.<sup>52</sup> Little is known about the antiangiogenesis ability of this compound. Herein, we clearly showed that melanin in the form of NPs inhibited angiogenesis in vitro. This characteristic could contribute to the role of melanin NPs as anticancer compounds. Remarkably, our study indicated the radiation resistance of UCMSCs at both cellular and molecular levels. Radiation did not affect cell viability or functional genes in UCMSCs, such as VEGF-A, SOD, Caspase-3, and IL-1 $\alpha$ . In addition, the differentiation ability of MSCs was maintained after X-ray exposure, especially for osteogenesis and adipogenesis. The radiation resistance feature of UCMSCs was consistent with previous studies.<sup>53,54</sup> It is worth noting that most of these published papers concentrated on the radioprotective activity of MSCs in gamma ray irradiation. In our study, we demonstrated the X-ray resistance of this cell type.

The zebrafish embryo model is considered the most suitable for the toxicity assessment of medical compounds in the early development phase.<sup>55</sup> In this study, after 96 h of treatment with melanin NPs, the TI values were kept from 0.7 to 1, indicating that melanin NPs were a teratogenic substance and safe for embryo development under the ICH S5(R3) Guideline.<sup>55</sup> The in vivo radiation-protective activity of melanin NPs was also investigated in a zebrafish embryo model. However, the embryo viability was still high, even at the highest tested dose of 15 Gy. Of note, the dose (15 Gy) used in the study was 10 times higher than the dose applied to humans<sup>37</sup> but was still unable to affect the embryo. A higher

dose should be used in a further work to determine the protective effect of melanin NPs. Nevertheless, the results indicated that melanin NPs were not synergistic with irradiation and were lethal to zebrafish embryos.

However, our study also had some limitations, suggesting that further work should be addressed. First, the quantitative relationship between the cellular melanin NP uptake and the cytotoxicity should be measured. Second, the involvement of the NP distribution and its radioprotective activity should be studied. Third, the mechanism of NP aggregation in the cell culture medium of hFBs and UCMSCs should be clarified. Furthermore, from what we have found, the follow-up in vivo experiments should be designed to verify selective protection of different cell types within the organism. Nonetheless, these results still suggested that squid-ink-derived melanin NPs play a potential role as a cell-type selective radiation-protective agent.

## 5. CONCLUSIONS

In conclusion, squid ink melanin NPs showed the highest biocompatibility and X-ray protective activity in human fibroblasts but affected the function of hUVECs. These NPs could inhibit the tube formation and migration of hUVECs. Even though the NPs showed no effect on the early development of the zebrafish embryo, the use of nanomelanin on targeted cells should be carefully investigated and controlled.

## AUTHOR INFORMATION

### Corresponding Author

**Nhung-Thi My Hoang** – VNU University of Science, Vietnam National University, Hanoi 10000, Vietnam; Center of Applied Sciences, Regenerative Medicine and Advanced Technologies, Vinmec Healthcare System, Hanoi 10000, Vietnam; [orcid.org/0000-0003-1717-1570](https://orcid.org/0000-0003-1717-1570); Email: [hoangthimynhung@hus.edu.vn](mailto:hoangthimynhung@hus.edu.vn)

### Authors

**Le-Na Thi Nguyen** – VNU University of Science, Vietnam National University, Hanoi 10000, Vietnam  
**Xuan-Hai Do** – Vietnam Military Medical University, Hanoi 10000, Vietnam  
**Hanh B. Pham** – VNU University of Science, Vietnam National University, Hanoi 10000, Vietnam  
**Dinh Duy-Thanh** – VNU University of Science, Vietnam National University, Hanoi 10000, Vietnam; [orcid.org/0000-0002-4346-4150](https://orcid.org/0000-0002-4346-4150)  
**Uyen Thi Trang Than** – Vinmec HiTech Center & Vinmec-VinUni Institute of Immunology, Vinmec Healthcare System, Hanoi 10000, Vietnam  
**Thu-Huyen Nguyen** – VinMec-VinUni Institute of Immunology, Vinmec Healthcare System, Hanoi 10000, Vietnam  
**Van-Ba Nguyen** – Vietnam Military Medical University, Hanoi 10000, Vietnam  
**Duc-Son Le** – VNU University of Science, Vietnam National University, Hanoi 10000, Vietnam  
**Dinh-Thang Nguyen** – VNU University of Science, Vietnam National University, Hanoi 10000, Vietnam; Present Address: VNU Vietnam Japan University, Vietnam National University, Hanoi 10000, Vietnam  
**Kien Trung Kieu** – VNU University of Science, Vietnam National University, Hanoi 10000, Vietnam

**Phuc Trong Nguyen** – Vietnam Military Medical University, Hanoi 10000, Vietnam  
**Manh Duc Vu** – Vietnam Military Medical University, Hanoi 10000, Vietnam  
**Nghia Trung Tran** – VNU University of Science, Vietnam National University, Hanoi 10000, Vietnam  
**Thanh Lai Nguyen** – VNU University of Science, Vietnam National University, Hanoi 10000, Vietnam  
**Lien T H Nghiem** – Institute of Physics, Vietnam Academy of Science and Technology, Hanoi 10000, Vietnam  
**Toan D. Nguyen** – Institute of Physics, Vietnam Academy of Science and Technology, Hanoi 10000, Vietnam  
**Nga Thi Hang Nguyen** – Thuyloi University, Hanoi 10000, Vietnam

Complete contact information is available at:  
<https://pubs.acs.org/10.1021/acsomega.3c09351>

### Author Contributions

L.-N.T.N. contributed to conception and design, manuscript writing, and revision; X.-H.D. contributed to partial concept and design, experiment performance, data analysis, and manuscript writing; H.B.P., M.D.V., and P.T.N. contributed to experiment performance (cell culture, cell viability assay, and cell senescence assay) and data analysis; T.H.N. and U.T.T.T. contributed to experiment performance (tube formation assay) and manuscript writing; V.-B.N. contributed to experiment performance (irradiation assay) and data analysis; D.-S.L. contributed to experiment performance (RT-PCR) and data analysis. L.-N.T.N., D.D.-T., T.L.N., and K.T.K. contributed to experiment performance (toxicity test on the Zebrafish larvae) and analysis; L.-N.N.T., T.D.N., and N.T.H.N. contributed to experiment performance (nanoparticle synthesis and characterization); N.T.T., D.-T.N., and L.T.H.N. contributed to the conception, provision of study material, and manuscript revision; N.-T.M.H. contributed to the concept and design, financial support, data analysis, and manuscript writing. The authors read and approved the final manuscript.

### Funding

This work was supported by the Vingroup Innovation Foundation, grant number VINIF.2020.DA07.

### Notes

The authors declare no competing financial interest.

### ACKNOWLEDGMENTS

The authors thank Dieu-Linh Do, Xuan Phuong Thi Do, and Quang Minh Nguyen for their technical assistance in cell viability, wound healing, cell differentiation, angiogenesis, and RT-PCR assays. We also thank Nguyen Manh Khai for his support in the irradiation procedure. We thank Assoc. Prof. Thu Thi Vu and Assoc. Prof. Nam Hoang Nguyen for their advice on manuscript preparation.

### REFERENCES

- (1) Costin, G.-E.; Hearing, V. J. Human skin pigmentation: melanocytes modulate skin color in response to stress. *FASEB journal*. **2007**, *21*, 976–994.
- (2) Miao, Y.; Sheng, J.; Wang, X.; Shi, C.; Sun, Q.; Liu, T.; et al. Melanin nanoparticles as an actinide in vivo sequestration agent with radiation protection effect. *New J. Chem.* **2021**, *45*, 9518–9525.
- (3) Kan, H.; Kim, C.-H.; Kwon, H.-M.; Park, J.-W.; Roh, K.-B.; Lee, H.; et al. Molecular Control of Phenoxidase-induced Melanin Synthesis in an Insect\*◆. *J. Biol. Chem.* **2008**, *283*, 25316–25323.
- (4) Hong, Z.-Y.; Feng, H.-Y.; Bu, L.-H. Melanin-based nanomaterials: The promising nanoplatforams for cancer diagnosis and therapy. *Nanomedicine: Nanotechnology, Biology and Medicine*. **2020**, *28*, No. 102211.
- (5) Kunwar, A.; Adhikary, B.; Jayakumar, S.; Barik, A.; Chattopadhyay, S.; Raghukumar, S.; et al. Melanin, a promising radioprotector: Mechanisms of actions in a mice model. *Toxicology and applied pharmacology*. **2012**, *264*, 202–211.
- (6) Rageh, M. M.; El-Gebaly, R. H.; Abou-Shady, H.; Amin, D. G. Melanin nanoparticles (MNPs) provide protection against whole-body  $\gamma$ -irradiation in mice via restoration of hematopoietic tissues. *Molecular and cellular biochemistry*. **2015**, *399*, 59–69.
- (7) Dong, J.; Sun, J.; Cai, W.; Guo, C.; Wang, Q.; Zhao, X.; et al. A natural cuttlefish melanin nanoprobe for preoperative and intraoperative mapping of lymph nodes. *Nanomedicine: Nanotechnology, Biology and Medicine*. **2022**, *41*, No. 102510.
- (8) Le Na, N. T.; Duc Loc, S.; Minh Tri, N. L.; Bich Loan, N. T.; Anh Son, H.; Linh Toan, N.; et al. Nanomelanin Potentially Protects the Spleen from Radiotherapy-Associated Damage and Enhances Immunoactivity in Tumor-Bearing Mice. *Materials*. **2019**, *12*, 1725.
- (9) Le Na, N. T.; Van Khanh, B. T.; Xuan Huy, P.; Nhung, H. T. M.; Thi Van Anh, N.; Thang, N. D. Melanin biomaterial effectively eliminates bacteria from water and synergistically induces melanoma-cell death during X-ray irradiation. *Materials Technology*. **2021**, *36*, 261–269.
- (10) Pacelli, C.; Bryan, R. A.; Onofri, S.; Selbmann, L.; Shuryak, I.; Dadachova, E. Melanin is effective in protecting fast and slow growing fungi from various types of ionizing radiation. *Environmental microbiology*. **2017**, *19*, 1612–1624.
- (11) Poulouse, N.; Sajayan, A.; Ravindran, A.; Sreechithra, T. V.; Vardhan, V.; Selvin, J.; et al. Photoprotective effect of nanomelanin-seaweed concentrate in formulated cosmetic cream: With improved antioxidant and wound healing properties. *Journal of Photochemistry and Photobiology B: Biology*. **2020**, *205*, No. 111816.
- (12) Berg, T. J.; Pietras, A. *Radiotherapy-induced remodeling of the tumor microenvironment by stromal cells*. *Seminars in cancer biology*; Elsevier: 2022.
- (13) Dormand, E.-L.; Banwell, P. E.; Goodacre, T. E. Radiotherapy and wound healing. *International wound journal*. **2005**, *2*, 112–127.
- (14) Chan, C. K.; Gulati, G. S.; Sinha, R.; Tompkins, J. V.; Lopez, M.; Carter, A. C.; et al. Identification of the human skeletal stem cell. *Cell* **2018**, *175* (1), 43–56.e21.
- (15) Spees, J. L.; Lee, R. H.; Gregory, C. A. Mechanisms of mesenchymal stem/stromal cell function. *Stem Cell Res. Ther.* **2016**, *7*, 125.
- (16) Soundararajan, M.; Kannan, S. Fibroblasts and mesenchymal stem cells: Two sides of the same coin? *Journal of cellular physiology*. **2018**, *233*, 9099–109.
- (17) Rafii, S.; Butler, J. M.; Ding, B.-S. Angiocrine functions of organ-specific endothelial cells. *Nature*. **2016**, *529*, 316–25.
- (18) Venkatesulu, B. P.; Mahadevan, L. S.; Aliru, M. L.; Yang, X.; Bodd, M. H.; Singh, P. K.; et al. Radiation-induced endothelial vascular injury: a review of possible mechanisms. *JACC: Basic and Translational Science*. **2018**, *3*, 563–72.
- (19) Kosmacek, E. A.; Oberley-Deegan, R. E. Adipocytes protect fibroblasts from radiation-induced damage by adiponectin secretion. *Sci. Rep.* **2020**, *10*, 12616.
- (20) Dulong, J.; Kouakou, C.; Mesloub, Y.; Rorteau, J.; Moratille, S.; Chevalier, F. P.; et al. NFATC2 Modulates Radiation Sensitivity in Dermal Fibroblasts From Patients With Severe Side Effects of Radiotherapy. *Front Oncol.* **2020**, *10*, No. 589168.
- (21) Cmielova, J.; Havelek, R.; Soukup, T.; Jiroutová, A.; Visek, B.; Suchánek, J.; et al. Gamma radiation induces senescence in human adult mesenchymal stem cells from bone marrow and periodontal ligaments. *International journal of radiation biology*. **2012**, *88*, 393–404.
- (22) Singh, S.; Bhaduri, A.; Tripathi, R. K.; Thapa, K. B.; Kumar, R.; Yadav, B. C. Improved sensing behavior of self-healable solar light

- photodetector based on core-shell type Ni<sub>0.2</sub>Zn<sub>0.8</sub>Fe<sub>2</sub>O<sub>4</sub>@ poly (Urea-Formaldehyde). *Solar Energy*. **2019**, *188*, 278–90.
- (23) Wang, K.-X.; Cui, W.-W.; Yang, X.; Tao, A.-B.; Lan, T.; Li, T.-S.; et al. Mesenchymal stem cells for mitigating radiotherapy side effects. *Cells*. **2021**, *10*, 294.
- (24) Chapel, A.; Francois, S.; Douay, L.; Benderitter, M.; Voswinkel, J. New insights for pelvic radiation disease treatment: multipotent stromal cell is a promise mainstay treatment for the restoration of abdominopelvic severe chronic damages induced by radiotherapy. *World journal of stem cells*. **2013**, *5*, 106.
- (25) Kursova, L. V.; Konoplyannikov, A. G.; Pasov, V. V.; Ivanova, I. N.; Poluektova, M. V.; Konoplyannikova, O. A. Possibilities for the use of autologous mesenchymal stem cells in the therapy of radiation-induced lung injuries. *Bulletin of experimental biology and medicine*. **2009**, *147*, 542–6.
- (26) Portas, M.; Mansilla, E.; Drago, H.; Dubner, D.; Radl, A.; Coppola, A.; et al. Use of human cadaveric mesenchymal stem cells for cell therapy of a chronic radiation-induced skin lesion: A case report. *Radiation protection dosimetry*. **2016**, *171*, 99–106.
- (27) Sokolov, M.; Neumann, R. Changes in gene expression as one of the key mechanisms involved in radiation-induced bystander effect. *Biomed. Rep.* **2018**, *9*, 99–111.
- (28) Tian, L.; Li, X.; Ji, H.; Yu, Q.; Yang, M.; Guo, L.; et al. Melanin-like nanoparticles: advances in surface modification and tumor photothermal therapy. *J. Nanobiotechnol.* **2022**, *20*, 1–29.
- (29) Pezzella, A.; Barra, M.; Musto, A.; Navarra, A.; Alfe, M.; Manini, P.; et al. Stem cell-compatible eumelanin biointerface fabricated by chemically controlled solid-state polymerization. *Materials Horizons*. **2015**, *2*, 212–20.
- (30) Bettinger, C. J.; Bruggeman, J. P.; Misra, A.; Borenstein, J. T.; Langer, R. Biocompatibility of biodegradable semiconducting melanin films for nerve tissue engineering. *Biomaterials*. **2009**, *30*, 3050–7.
- (31) Piacenti-Silva, M.; Matos, A. A.; Paulin, J. V.; Alavarce da Silva, R. A.; de Oliveira, R. C.; Graeff, C. F. Biocompatibility investigations of synthetic melanin and melanin analog for application in bioelectronics. *Polym. Int.* **2016**, *65*, 1347–1354.
- (32) Gabriele, V. R.; Mazhabi, R. M.; Alexander, N.; Mukherjee, P.; Seyfried, T. N.; Nwaji, N.; et al. Light-and melanin nanoparticle-induced cytotoxicity in metastatic cancer cells. *Pharmaceutics*. **2021**, *13*, 965.
- (33) Freilikhman, S.; Halasi, M.; Eran, A.; Adini, I. Melanocytes determine angiogenesis gene expression across human tissues. *Plos one*. **2021**, *16*, No. e0251121.
- (34) Guangqi, E.; Cao, Y.; Bhattacharya, S.; Dutta, S.; Wang, E.; Mukhopadhyay, D. Endogenous vascular endothelial growth factor-A (VEGF-A) maintains endothelial cell homeostasis by regulating VEGF receptor-2 transcription. *J. Biol. Chem.* **2012**, *287*, 3029–3041.
- (35) Rogers, K. J.; Shtanko, O.; Vijay, R.; Mallinger, L. N.; Joyner, C. J.; Galinski, M. R.; et al. Acute plasmodium infection promotes interferon-gamma-dependent resistance to Ebola virus infection. *Cell reports*. **2020**, *30*, 4041–51.
- (36) Zhu, J.-W.; Ni, Y.-J.; Tong, X.-Y.; Guo, X.; Wu, X.-P. Activation of VEGF receptors in response to UVB promotes cell proliferation and melanogenesis of normal human melanocytes. *Exp. Cell Res.* **2020**, *387*, No. 111798.
- (37) Braunbeck, T. *Fish Embryo Acute Toxicity (FET) Test*; Oecd Publishing: 2013.
- (38) Nations U. *Globally harmonized system of classification and labeling of chemicals (GHS)*; United Nations: New York, NY, USA, 2011.
- (39) Wiegand, C.; Hipler, U.-C. Evaluation of Biocompatibility and Cytotoxicity Using Keratinocyte and Fibroblast Cultures. *Skin Pharmacol Physiol*. **2009**, *22*, 74–82.
- (40) Baar, M. P.; Brandt, R. M.; Putavet, D. A.; Klein, J. D.; Derks, K. W.; Bourgeois, B. R.; et al. Targeted apoptosis of senescent cells restores tissue homeostasis in response to chemotoxicity and aging. *Cell* **2017**, *169* (1), 132–147.e16.
- (41) Rhinn, M.; Ritschka, B.; Keyes, W. M. Cellular senescence in development, regeneration and disease. *Development* **2019**, *146*, dev151837.
- (42) Yan, J.; Wang, J.; Huang, H.; Huang, Y.; Mi, T.; Zhang, C.; et al. Fibroblast growth factor 21 delayed endothelial replicative senescence and protected cells from H<sub>2</sub>O<sub>2</sub>-induced premature senescence through SIRT1. *Am. J. Transl. Res.* **2017**, *9*, 4492.
- (43) Kontos, C. D. More than skin deep: connecting melanocyte pigmentation and angiogenic diseases. *Journal of clinical investigation*. **2014**, *124*, 76–9.
- (44) Han, H.; Kim, Y.; Mo, H.; Choi, S. H.; Lee, K.; Rim, Y. A.; et al. Preferential stimulation of melanocytes by M2 macrophages to produce melanin through vascular endothelial growth factor. *Sci. Rep.* **2022**, *12*, 6416.
- (45) Ji, S.; Dong, W.; Qi, Y.; Gao, H.; Zhao, D.; Xu, M.; et al. Phagocytosis by endothelial cells inhibits procoagulant activity of platelets of essential thrombocythemia in vitro. *Journal of Thrombosis and Hemostasis*. **2020**, *18*, 222–33.
- (46) Lee, H.; Sodek, K. L.; Hwang, Q.; Brown, T. J.; Ringuelette, M.; Sodek, J. Phagocytosis of collagen by fibroblasts and invasive cancer cells is mediated by MT1-MMP. *Biochem. Soc. Trans.* **2007**, *35*, 704–6.
- (47) Zhang, Z.; Huang, S.; Wu, S.; Qi, J.; Li, W.; Liu, S.; et al. Clearance of apoptotic cells by mesenchymal stem cells contributes to immunosuppression via PGE<sub>2</sub>. *EBioMedicine*. **2019**, *45*, 341–50.
- (48) Baselet, B.; Sonveaux, P.; Baatout, S.; Aerts, A. Pathological effects of ionizing radiation: endothelial activation and dysfunction. *Cellular and molecular life sciences*. **2019**, *76*, 699–728.
- (49) Nhan, T. T.; Matuo, Y.; Abdillah, M.; Wicaksono, L. W.; Izumi, Y. Ascorbic Acid as a Radiation-Protective Agent Against Ionizing Radiation. 8th International Conference on the Development of Biomedical Engineering in Vietnam: Proceedings of BME 8, 2020, Vietnam: Healthcare Technology for Smart City in Low-and Middle-Income Countries. *Springer* **2022**, *85*, 845–57.
- (50) Ushakov, I. B.; Vasin, M. V. Radiation protective agents in the radiation safety system for long-term exploration missions. *Human Physiology*. **2014**, *40*, 695–703.
- (51) Vasin, V. M. The classification of radiation protective agents as the reflection of the present state and development perspective, of current radiation pharmacology. *Radiats. Biol., Radioecol.* **2013**, *53*, 459–467.
- (52) Marcovici, I.; Coricovac, D.; Pinzaru, I.; Macasoi, I. G.; Popescu, R.; Chioibas, R.; et al. Melanin and melanin-functionalized nanoparticles as promising tools in cancer research—a review. *Cancers*. **2022**, *14*, 1838.
- (53) He, X.; Sun, J.; Zhuang, J.; Xu, H.; Liu, Y.; Wu, D. Microneedle system for transdermal drug and vaccine delivery: devices, safety, and prospects. *Dose Response* **2019**, *17*, No. 1559325819878585.
- (54) Nicolay, N. H.; Sommer, E.; Lopez, R.; Wirkner, U.; Trinh, T.; Sisombath, S.; et al. Mesenchymal stem cells retain their defining stem cell characteristics after exposure to ionizing radiation. *International Journal of Radiation Oncology\* Biology\**. **2013**, *87*, 1171–8.
- (55) Song, Y.-S.; Dai, M.-Z.; Zhu, C.-X.; Huang, Y.-F.; Liu, J.; Zhang, C.-D.; et al. Validation, optimization, and application of the zebrafish developmental toxicity assay for pharmaceuticals under the ICH S5 (R3) guideline. *Frontiers in cell and developmental biology*. **2021**, *9*, No. 721130.